Mobile Integrons Encode Phage Defence Systems

Nicolas KIEFFER[1,2], Alberto HIPÓLITO[1,2], Paula BLANCO[1,2], Thomas DELOBELLE[3], Francisco Manuel OJEDA[1,2], Thomas JOVÉ[4], Dukas JURENAS[3], Meritxell GARCÍA-QUINTANILLA[5,6], Pilar DOMINGO-CALAP[7], José Antonio ESCUDERO[1,2*]

[1]Molecular basis of Adaptation Laboratory, Departamento de Sanidad Animal, Facultad de Veterinaria de la Universidad Complutense de Madrid, Madrid, España,

[2]VISAVET Health Surveillance Centre, Universidad Complutense de Madrid, Spain.

[3] Laboratoire de Génétique et Physiologie Bactérienne, Faculté de Sciences, Université Libre de Bruxelles (ULB), Gosselies, Belgium.

[4]INSERM, CHU Limoges, RESINFIT, University of Limoges, Limoges, France, Present address: no longer employed by INSERM.

[5]Departamento de Microbiología, Instituto de Investigación Sanitaria Fundación Jiménez Díaz, Madrid, España

[6]CIBERINFEC-CIBER de Enfermedades Infecciosas, Instituto de Salud Carlos III, Madrid, Spain

[7]Instituto de Biología Integrativa de Sistemas, Universitat de València-CSIC, Paterna, Spain.

*Corresponding Author. Email: jaescude@ucm.es

+34 661584761

University Complutense of Madrid,

Department of Animal Health,

Avenida Puerta de Hierro s/n

28040, Madrid, Spain.

ABSTRACT

Integrons are bacterial genetic elements that capture, stockpile and modulate the expression of genes encoded in integron cassettes. Mobile Integrons (MI) are borne on plasmids, acting as a vehicle for hundreds of antimicrobial resistance genes among key pathogens. These elements also carry gene cassettes of unknown function (*gcu*s) whose role and adaptive value remains unexplored. Recent years have witnessed the discovery of a myriad defence systems against bacteriophages, highlighting that viral infection is a major selective pressure for bacteria. We hence sought to explore if *gcu*s could encode phage defence systems. Using the INTEGRALL database, we established a collection of 129 *gcu*s in pMBA, a vector where cassettes are established as part of a class 1 integron. PADLOC and DefenseFinder predicted four phage defence systems in this collection, comprising Lamassu, CBASS and two ABI (abortive infection) systems. We experimentally challenged all cassettes with phages and found nine additional candidates that were not detected *in silico*. We have characterized in depth the 13 *gcu*s against a panel of phages in *Escherichia coli* confirming their role as phage defence integron cassettes (PICs). We used recombination assays to verify that all systems are *bona fide* integron cassettes and are therefore mobile. We show that PICs confer resistance in other clinically relevant species, such as *Klebsiella pneumoniae* and *Pseudomonas aeruginosa.* Several PICs also limit prophage activation, providing protection at the population-level. Given the stockpiling capacity of integrons, we explored the additivity of phenotypes and found that integrons with two PICs confer multiphage-resistance. Additionally, when combined with antimicrobial resistance genes, integrons confer simultaneously drug and phage resistance. Crucially, we also show that the position of a *pic* in the array can strongly decrease its cost. Our results prove a role of integrons in phage defence, acting as highly mobile, low-cost defence islands. This has important implications in the spread of defence systems, and on the future of phage therapy.

54 **INTRODUCTION**

55 Antimicrobial resistance (AMR) is a major public health concern worldwide, and the
56 emergence of multi-drug (MDR) resistant bacteria is making increasingly difficult to treat
57 infections with antibiotics[1]. Alternative therapeutic options are being explored as potential
58 solutions to this problem. Phage therapy -the use of viruses that infect and kill bacteria- is an
59 old approach (it predates the use of antibiotics) that is currently being revisited and building
60 momentum. Several recent reports have yielded positive results for the treatment of life-
61 threatening infections caused by MDR bacteria[2–4]. However, the efficacy of phage therapy can
62 be limited by the emergence of phage-resistant bacteria[5,6]. Resistance can typically emerge
63 through mutations in which the receptors recognized by the phage are lost, or through the
64 acquisition of defence systems. In recent years, a plethora of new defence systems have been
65 discovered and characterized to varying extents, adding to the classic restriction-modification
66 enzymes or the more modern CRISPR-Cas immune systems[7]. These can be classified according
67 to the mechanism used to sense phage infection into systems that detect nucleic acids, phage
68 proteins, the integrity of the host, and others[8,9]. These defence mechanisms have evolved in
69 response to phage predation, and they are often encoded in the vicinity of other systems,
70 creating defence islands. In fact, it was the proximity to known defence systems that allowed
71 the initial discovery of systems such as Lammasu, Kiwa, Thoeris, or Zorya, using a guilt-by-
72 association rationale[10–12]. Ever since, we have witnessed a sheer increase in the discovery of
73 novel defence systems. Their abundance in genomes illustrates the ongoing evolutionary arms
74 race between bacteria and their phages and highlights the importance of phage predation as a
75 selective pressure for bacteria[13]. Defence systems have been shown to be encoded in mobile
76 genetic elements such as integrative conjugative elements, transposons, or prophages[13].
77 However, they are proven to impact the fitness of the bacterial strains carrying them due to the
78 constitutive expression of their genetic content[14] highlighting the cost of resistance.

79 Integrons are genetic elements that play an important role in bacterial adaptation to
80 changing environmental conditions[15–17]. They capture and accumulate new genes embedded in
81 integron cassettes (ICs), acting as genetic memories of adaptive functions[18]. Integrons typically
82 consist of a conserved platform encoding the integrase gene and the recombination site in the
83 integron (*attI*)[19]; and a variable region containing the cassettes. Cassettes are incorporated into
84 the *attI* site through site-specific recombination reactions mediated by the integrase and are
85 expressed from the dedicated Pc promoter encoded in the platform[20]. The integrase can also
86 reorder cassettes in the array to modulate their expression, modifying their distance to the Pc

and the polar effects they are subjected to[21–23]. The expression of the integrase is controlled by the SOS response, so that integrons provide to their hosts "adaptation on demand"[24,25].

Mobile integrons (MI) are a subset of integrons that are typically associated with mobile genetic elements, such as plasmids and transposons, which can facilitate their horizontal transfer between bacterial cells[26–28]. They are a palpable example of the evolvability these platforms confer to their hosts. They were initially discovered in the first MDR isolates of *Shigella* spp. during the 1950's, carrying two resistance genes[29,30]. Nowadays MIs are commonplace among key Gram-negative pathogens[31] carrying almost 200 resistance genes against most antibiotic families[32–34]. Consequently, MIs are generally considered to be devoted almost exclusively to AMR. Nevertheless, among the cassettes found within MIs are gene cassettes of unknown function (*gcu*) whose importance has generally been overlooked[35]. Yet the working model of integrons suggests that cassettes must be adaptive at the time of integration when they are expressed at the maximum strength[24]. We hence reasoned that *gcu*s could be playing an unknown adaptive role. Given the importance of phage predation in the lifestyle of bacteria and in their genome's content, we sought to explore the possibility that *gcus* encode phage defence systems.

Here we have selected 129 *gcus* from the INTEGRALL database[36], and cloned them in pMBA, a plasmid mimicking the genetic environment of a mobile integron[37]. DefenseFinder[38] and PADLOC[39] predicted 4 *gcus* in the collection as potential defence systems. We then used *in vitro* screening test using phages T4 and T7 combined with structural prediction using AlphaFold and discovered 9 novel defence systems that were not predicted. All cassettes confer resistance to at least one of a panel of 8 phages against *E. coli*. We have confirmed that all systems are encoded in *bona fide* (functional) integron cassettes, which we have named Phage defence Integron Cassettes (PICs), and are hence mobile and likely to circulate among other species. Indeed, we demonstrate that they also confer resistance in *K. pneumoniae* and *P. aeruginosa,* major pathogens of the ESKAPEE group. As part of an integron, cassettes can be stockpiled in an array. Building arrays we show that phenotypes of PICs are additive, conferring multi-phage or phage/drug resistance if combined with other PICs or antimicrobial resistance cassettes (ARCs). We also show that the position of a PIC in the array can strongly diminish its cost. Altogether, our work proves the involvement of integrons in phage defence, acting as repositories of a broad variety of defence systems i.e.: as mobile and low-cost defence islands.

121 **RESULTS**

122 **Integron *gcus* contain predicted phage defence systems.**

123 To obtain a broad set of *gcu*s in MIs we screened the INTEGRALL database, the largest
124 repository for mobile integron-related data (date: November 2021). We retrieved 303 cassettes
125 annotated as *gcu*s (< 95% nucleotide identity) with sizes ranging from 191 bp to 3 kb. We
126 further analysed and curated this list manually using BLAST. We discarded several cassettes
127 misannotated as *gcu*s in which an insertion sequence had interrupted a cassette of known
128 function. Additionally, gene-less cassettes -that failed to produce hits with any known or
129 unknown protein- were also discarded. We therefore selected a panel of 129 elements with sizes
130 ranging from 284 to 2.950 bp (Figure S1). All elements were synthesized *in vitro* and cloned in
131 pMBA, a vector providing a biologically sound genetic environment, where cassettes are
132 inserted in first position of a class 1 integron and are under the control of a strong Pc promoter
133 (PcS)[40]. The sequences of our selected collection were submitted in May 2022 to the two major
134 web platforms specialized in phage resistance gene prediction, DefenseFinder and
135 PADLOC[38,39]. As a result of this computational analysis, we identified four distinct gene
136 cassettes (*gcu*s 59, 128, 135 and N) as potential defence mechanisms, each exhibiting homology
137 to a known system involved in phage resistance (Figure 1A).

138 Given their newly identified putative function as phage resistance elements, we propose
139 to rename these *gcus* as *pic*s, while conserving their numbers for simplicity. Pic59 (formerly
140 Gcu59) was identified as a homolog of the AriAB system[41] and is suggested to confer phage
141 resistance through abortive infection. *pic128* encodes two ORFs (*pic128A* and *pic128B*) and
142 shows similarity to a Lamassu Type 1 system. AlphaFold predicts that Pic128A shares motifs
143 with YfjL-like or AbpA proteins, which are involved in phage defence, while Pic128B contains
144 a putative exonuclease domain. Interestingly, the three-dimensional structure of Pic128B
145 protein displays a remarkable similarity to DdmC, a protein from the Lamassu Type 2 plasmid
146 and phage defence system described in *Vibrio cholerae*[42]. *pic135* also contains two ORFs and
147 share structural similarity with a CBASS Type 1 system[43]. The proteins encoded by this cassette,
148 Pic135A and Pic135B, are predicted to play roles in nucleotidyl-transfer and membrane
149 translocation, respectively, as suggested by protein structure predictions. Last, PicN is
150 annotated as an AbiV family protein[44], implicated in phage resistance through abortive infection
151 mechanisms.

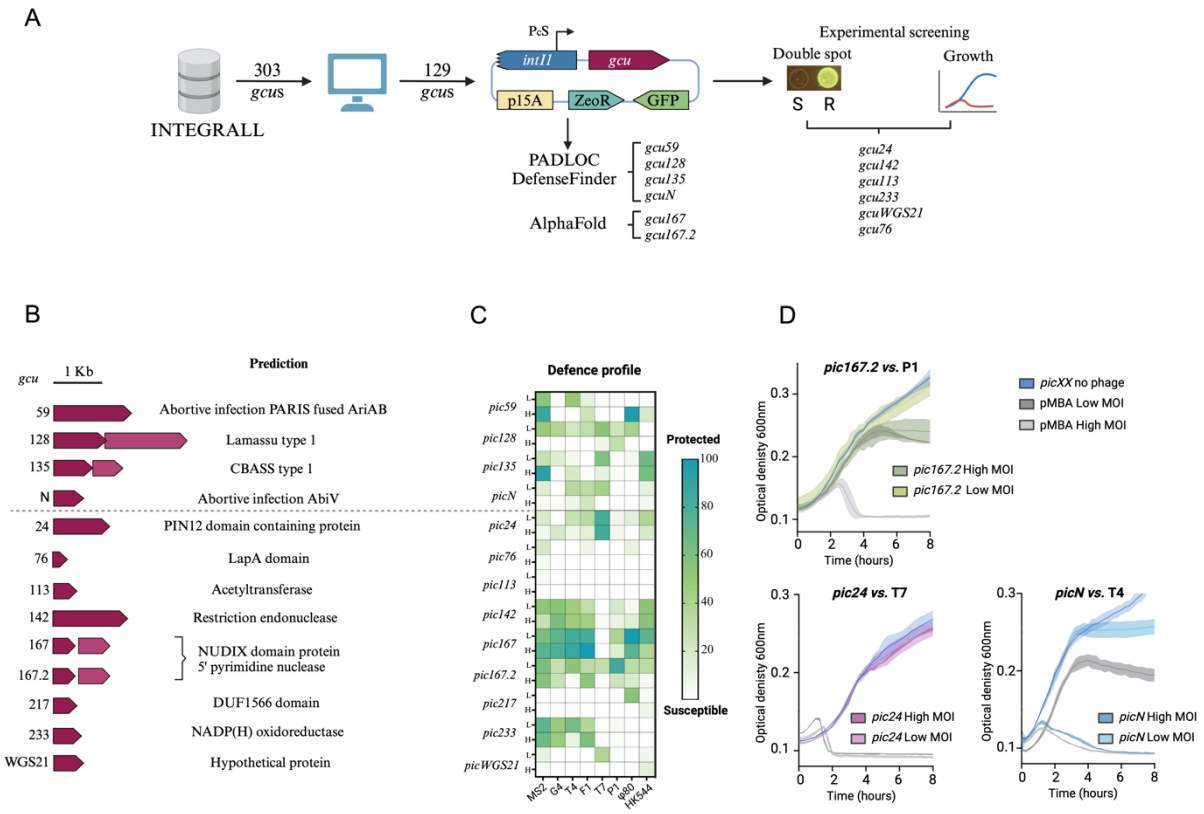

Figure 1. Identification and Characterization of Phage Defense Systems in Integron Cassettes. (A) Schematic workflow for the identification and experimental validation of phage defence systems in *gcus*. A collection of 303 gcus was extracted from the INTEGRALL database, curated to 129 *gcus*, and cloned into the pMBA vector, placing each *gcu* under the control of a strong integron promoter (PcS). Predicted phage defence systems were identified using PADLOC and DefenseFinder, (May 2022) and experimental screening was performed using a double-spot assay or growth curves to determine susceptibility or resistance to phage infection. **(B)** Genetic organization and predicted functions of selected *gcus*. Predicted function is shown for putative defence mechanisms and other candidate *gcus*. **(C)** Heatmap showing the defence profiles of identified Phage Integron Cassettes (PICs) against a panel of eight *E. coli* phages. The degree of protection (resistance) is indicated by the color scale, with dark green representing high protection, light green representing low protection, and white no protection. **(D)** Examples of growth curves used to build the heatmap in C, showing protective effects of selected PICs against different phages. (Top left) *pic167.2* confers resistance to phage P1 at both high and low multiplicities of infection (MOI). (Bottom left) *pic24* confers strong resistance to phage T7 at both high and low MOI. (Bottom right) *picN* shows resistance to phage T4 only at low MOI, characteristic of abortive infection mechanisms. Growth curves are represented as the mean of three independent replicates. The standard error of the mean is represented as a lighter colour shade.

Functional screening and domain prediction reveal additional phage defence systems.

Bioinformatic approaches can fail to detect novel systems that are not similar to any of the known ones. We hence turned to *in vitro* experiments to detect novel resistance mechanisms within our *gcu* collection. We employed a double spot screening protocol in solid media and the monitoring of growth curves in liquid media, to challenge the whole collection with different concentrations of phages T4 or T7 (Figure 1A and Figure S2). We successfully detected 7 new

175 candidates (*pic24, pic142*, *pic233, pic217, pic113, picWGS21* and *pic76*) presenting substantial
176 growth in the presence of phage (Figure S2). Using AlphaFold prediction model to find proteins
177 with potential nuclease domains, that are often linked to phage defence, we additionally
178 identified *pic167* and its close homolog *pic167.2*. *in silico* structural predictions of proteins
179 encoded in these PICs suggest a diversity of functional roles. Both Pic167 and Pic167.2 are
180 likely involved in nucleotide metabolism, with indications of NUDIX hydrolase and
181 nucleotidase activities. Pic142 is a putative restriction endonuclease, while Pic24 possesses a
182 PIN12 domain that potentially acts as a nuclease[45]. Pic233 is possibly a NADP(H)
183 oxidoreductase; Pic113 is a putative GNAT N-acetyltransferase and Pic217 a putative integral
184 membrane protein with a lectin C domain. AlphaFold did yield relevant homologs with a known
185 function for PicWGS21. Last, Pic76 is a small protein of 76 amino acid that contains a LapA
186 domain that has been related to biofilm formation[46] (Figure 1B).
187
188 **PICs confer protection to a panel of phages *Escherichia coli.***
189 To characterize in depth the role and profile of PICs in phage resistance, we subcloned
190 the whole library in strain *E. coli* IJ1862 (an F' strain that can be infected by plasmids targeting
191 the conjugative pilus[47]) and conducted infection assays with a panel of phages from different
192 families at varying multiplicities of infection (MOIs). We monitored the optical densities
193 (OD_{600}) over time of bacterial cultures in presence and absence of phage MS2, F1, G4, T4, T7,
194 P1, Φ80 and HK544. As a control, we included an isogenic strain carrying the empty vector
195 pMBA. We used the area under the (growth) curve to determine the protective effect of the
196 cassette, as in[48] (see Materials and Methods). Our data showed that all PICs conferred resistance
197 to at least one condition (one phage at one MOI) (Figure 1C and Figure S3), confirming their
198 role in phage defence. Resistance profiles were diverse, with some PICs showing broad-
199 spectrum resistance, such as *pic167, pic167.2*, *pic128* and *pic142*. Others, as *pic24,* showed a
200 narrower spectrum with low level resistance against several phages, but very high resistance
201 against phage T7 at both high and low MOI (Figure 1D). The resistance phenotype displayed
202 by *picN*, limited to low MOI for phages MS2, T4, F1 and T7, aligns with the characteristic
203 phenotype of an abortive infection, thereby confirming the predictions made by PADLOC and
204 DefenseFinder. Overall, our results confirm that the *gcus* identified in our screenings are indeed
205 phage resistance genes with known and characterized mechanisms.
206
207

208 **PICs are *bona fide* integron cassettes.**

209 Identification of integrons and their cassettes has not been a straightforward task until
210 the appearance of IntegronFinder[49]. A large part of the content in INTEGRALL predates
211 IntegronFinder, so their classification as integron cassettes needs to be verified. A close analysis
212 of the genetic context, locating integrases in close vicinity and in opposite orientation, can be
213 indirect proof that a gene is indeed a cassette. Most PICs identified here -except for *pic135* and
214 *pic142*- are located within class 1 or class 2 integrons, often in pathogenic strains belonging to
215 the *Enterobacteriaceae* family (like *pic217*, *pic113*, and *pic24*) or multidrug resistant *P.*
216 *aeruginosa.* A compelling example of the latter is the presence of *picN* next to cassettes $bla_{IMP,}$
217 *aacA4* and *catB6,* conferring multidrug resistance to carbapenems, aminoglycosides, and
218 chloramphenicol, respectively (Accession number: AJ223604) (Figure 2A). Yet, given that
219 finding defence systems in integrons has important implications for the mobility of these
220 systems, we sought to verify experimentally that these are *bona fide* integron cassettes. Cassette
221 recombination is a site-specific reaction that can be evidenced in a suicide conjugation assay
222 that is typical in the field[50,51]. Crucially, recombination is semiconservative, involving the
223 bottom strand (but not the top strand) of both the *attC* sites in cassettes and *attI* sites of integrons
224 [52,53]. This unique feature can be easily detected because it leads to clear differences in the suicide
225 conjugation assay when the plasmid transfers the bottom or top strand of the cassette[54]. With
226 this in mind, we inserted the putative *attC* sites of all *pics* in both orientations in the suicide
227 vector pSW23T and measured the recombination frequency of both strands for each cassette.
228 Recombination events were verified through PCR. As expected, we observed a clear drop
229 (between 100- and 10.000-fold lower) in the recombination frequency of the top strands of all
230 putative *attC* sites, as would be expected from integron cassettes (Figure 2B). *picWGS21* had
231 extremely low recombination frequencies for the bottom strand. Yet recombination of the top
232 strand was only observed in 1 out of 6 replicate experiments, suggesting that it is indeed an
233 integron cassette albeit with a very poor recombination site. Indeed, the folded *attC* site of
234 *picWGS21* the typical hairpin structure and Extra Helical Bases of these sites (Figure S4)[55–57].
235 Hence, our data confirms that PICs are *bona fide* integron cassettes.

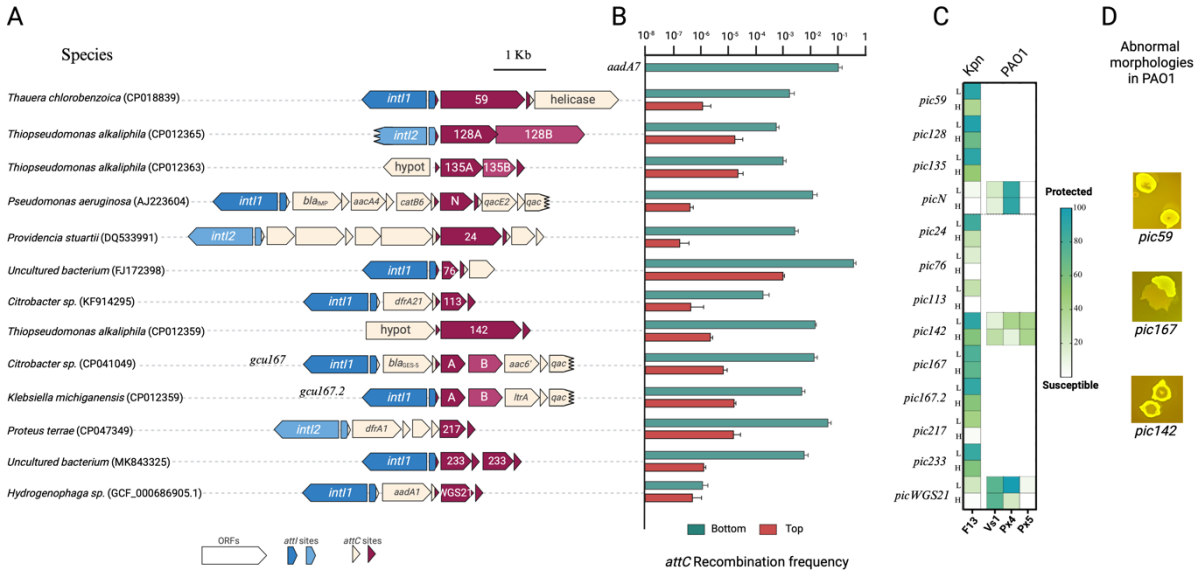

Figure 2. Genetic Context, Recombination Frequency, and Phage Protection Profiles of Identified PICs in other species. (A) Genetic context of PICs as found in databases, highlighting their association with integron integrases (*intI1* or *intI2*, in blue shades). PICs are found in different host species. Each PIC is annotated with its respective identifier (e.g., 59, 128A/B, 135A/B), along with known associated genes such as resistance genes (e.g., bla_{IMP}, *aacA4*, *catB6*). **(B)** Recombination frequency of the *attC* sites of the identified PICs. The recombination frequency was measured for the bottom (green bars) and top (red bars) strands of the attC sites using a suicide conjugation assay. A clear drop in the recombination frequency of the top strands compared to the bottom strands confirms that these *gcus* are *bona fide* integron cassettes. Bars represent the mean of at least 6 biological replicates. Error bars correspond to the standard error of the mean. **(C)** Heatmap showing the protection profiles of PICs against phage infection in different host species, including *K. pneumoniae* (Kp5) and *P. aeruginosa* (PAO1) against a panel of cognate phages (F13, Vs1, Px4, Px5).

Defence cassettes are protective in other species.

Given the mobility of integrons and cassettes among important pathogens, we sought to determine if PICs are active in different hosts. To this end, we evaluated the protective effects of PICs in *K. pneumoniae* and *P. aeruginosa,* two species of the ESKAPEE group of highly resistant and lethal pathogens where integrons are prevalent. We introduced all PICs into *K. pneumoniae* Kp5, a MDR clinical isolate. We sequenced the genome of this strain and found three plasmids, one of which contains a class 1 integron (full resistome can be found in Table S1). The PHASTEST software did not detect prophages in the genome of Kp5. We subjected all strains to infection with the *Drexlerviridae* phage F13 co-isolated with the strain. All PICs, except *picN*, demonstrated resistance to F13 at low MOI. Most of them also conferred resistance at high MOI (except *pic76*, *pic113*, *pic217*, and *picWGS21*) (Figure 2C). To introduce PICs in *P. aeruginosa* PAO1 strain, we changed the p15A origin of replication of pMBA for BBR1, and introduced a tetracycline resistance marker. After several assays, we could only transform *picN* successfully, while other PICs produced no colonies at all or abnormal (sick) colony morphologies (Figure 2D). This led us to hypothesize that some *pics* might be toxic or extremely costly in this background. To avoid this, we changed the strong promoter guiding the

263 expression of cassettes in pMBA (PcS) for a weaker version (PcW). This way we could
264 introduce *pic24, pic113, pic142* and *picWGS21* in PAO1 and were able to measure their
265 activities. We confronted these strains to a collection of 36 phages infecting PAO1 using a
266 double spot screen. We observed growth for *picN*, *pic142* and *picWGS21* in presence of phages
267 Vs1, Px4 and Px5. We evaluated the level of resistance by monitoring growth curves for each
268 PIC against the three phages, and confirmed their resistance phenotype (Figure 2C). *pic142* -
269 that had a clear phenotype against several phages both in *E. coli* and *K. pneumoniae*- confirmed
270 its broad spectrum and host range, conferring resistance to Px5 at both MOI and to Px4 at low
271 MOI ; contrarily, *picN* and *picWGS21,* that had only showed low resistance against a handful
272 of phages in *E. coli*, conferred very high resistance against phage Px4 and Vs1 in *P. aeruginosa*.
273 Altogether, our data proves that PICs can confer resistance to different phages and in different
274 host species. Although some PICs seem to have a defined narrow host range, others, like *pic142*
275 were able to confer resistance in the three species against most phages tested, underlying the
276 broad-spectrum activity of this defence mechanism.
277
278 **PICs protect against prophage activation.**
279 An important aspect of the interplay between phages, their hosts, mobile genetic
280 elements and defence systems is the case of prophage activation. Hindering activation of
281 prophages can both protect at the cell and at the population level. Here we asked if a plasmid
282 carrying a mobile integron with a PIC can limit the production of phage particles from a
283 chromosomally encoded prophage once it switches to lytic cycle. To test this, we used phages
284 HK544 and Φ80. We have previously found that *pic135*, *pic24, pic142, pic167* and *pic167.2*
285 confer resistance to the free form of phages HK544 at both MOI conditions and that *pic167,*
286 *pic167.2, pic128 and pic217* showed resistance to phage Φ80 at low MOI (Figure 1C). With
287 these results in mind, we then introduced a subset of these PICs in lysogens of *E. coli* 544 with
288 either HK544 or Φ80 prophages in their genomes. As a control, we also included *picN*, that did
289 not significantly protect against any of the free forms. We induced prophage activation with
290 mitomycin and quantitated the phage titer after 6 hours. We did not observe protection against
291 Φ80 reactivation in any of the four PICs tested, while *pic128*, *pic135* and *pic142* showed a 10
292 to 1.000 fold decrease in plaque forming units of HK544 (Figure 3A). Interestingly, while
293 *pic135* and *pic142* confer resistance against both free and prophage forms of HK544, *pic128*
294 only conferred resistance against prophage activation. These results show that mobile integrons
295 containing PICs can interfere with prophage activation, highlighting the potential protective
296 effect at the community level, and the complex interplay between mobile genetic elements.

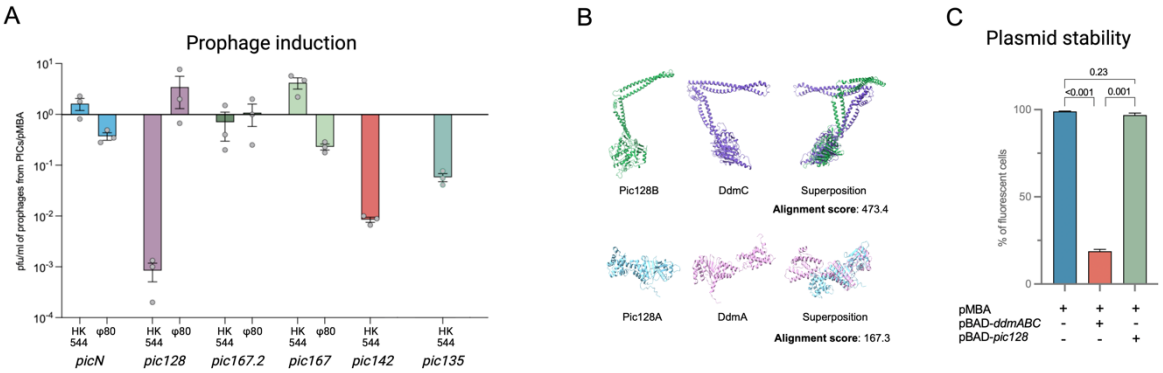

Figure 3. Prophage Induction, Structural Alignment, and Impact of *pic128* on Plasmid Stability. **(A)** Prophage induction assays inducing with mitomycin (0,05 µM). The graph shows the concentration of phage (measured as plaque-forming units per millilitre (pfu/ml)) when activating prophages in the presence of pMBA containing PICs (*picN*, *pic128*, *pic167.2*, *pic167*, *pic142*, *pic135*) over the presence of the empty pMBA vector. The results indicate that *pic128*, *pic135*, and *pic142* significantly decrease the phage titer of HK544, while no protection is observed for Φ80 prophage. **(B)** Structural alignment of Pic128A and Pic128B proteins with known phage and plasmid defence proteins DdmA and DdmC, respectively. Superposition of protein structures is shown, with alignment scores indicating the degree of structural similarity. **(C)** Plasmid stability assays in *E. coli*. The percentage of fluorescent cells, representing the stability of pMBA, is shown for strains containing the pBAD plasmid with either the *ddmABC* or *pic128AB* systems. While *ddmABC* significantly reduces plasmid stability, *pic128* does not show a significant effect, indicating no anti-plasmid activity. Bars represent the mean of at least 3 biological replicates. Error bars correspond to the standard error of the mean. Statistical significance was assessed through unpaired t-tests and p-values are shown.

pic128 does not have anti-plasmid activity.

DdmABC is a phage and plasmid defence system. It has been shown to confer phage resistance in *E. coli* and to cure plasmids in *Vibrio cholerae*, particularly those with a p15A replication origin[58]. When modelling protein structures of PICs, we found strong similarities between Pic128B and DdmC (Figure 3B), proteins that belong to (different) Lamassu defence systems. Interested by the interactions between mobile elements, we set out to examine whether the expression of *pic128AB* could exert a similar influence on plasmid stability. Because pMBA has a p15A replication origin, we decided to investigate the antiplasmid activity of *pic128AB* from a different vector. We hence cloned *pic128AB* and *ddmABC* systems into a pBAD plasmid that possess a pBR322 origin of replication and co-transformed them with an empty pMBA. We induced both systems with arabinose and monitored the loss of pMBA as the presence of non-fluorescent colonies for 3 days (ca. 20 generations). pMBA is stably maintained in the absence of antibiotics, with 99% of the cells in the population being fluorescent after 3 days. As expected, DdmABC strongly decreased the proportion of fluorescent colonies to 19% by day 3 (Figure 3C), while pMBA was stably maintained at >97% in the presence Pic128AB. This suggests that, despite their structural similarities, Pic128AB does not have the anti-plasmid activity detected for DdmABC. Still, both systems could have different plasmid specificities,

328 so we extended our plasmid stability studies to Kp5, carrying the three distinct natural plasmids
329 conferring resistance to tetracycline, ertapenem and cefotaxime, respectively. After introducing
330 pMBA-*pic128* into this isolate we assessed plasmid stability monitoring the loss of three
331 resistance phenotypes conferred by these replicons over a five-day period (Figure S5). We could
332 not observe a significant plasmid loss in any case, suggesting that *pic128* is not an anti-plasmid
333 system.
334
335 **Mobile Integrons can accumulate resistance to phages and antibiotics.**
336 The fact that integrons carry defence systems is important in the ecology and biology of
337 these systems. Integron cassettes can be stockpiled, and their phenotypes can be additive, as for
338 we have observed for multi-drug resistance MIs. It is hence possible that integrons can combine
339 PICs to provide multi-phage resistance; or PICs and antimicrobial resistance cassettes (ARCs)
340 providing phage- and AMR. This is important for phage therapy, since integrons would likely
341 play again -as it occurred with antibiotics- a key role in the evolution of resistance. Hence, we
342 sought to test if phage defence phenotypes can be additive and combined with antimicrobial
343 resistance genes. To do so, we first constructed pArray-1 an integron combining *pic24* and
344 *pic167.2* (Figure 4A) that confer high and intermediate resistance to phage T7 and P1,
345 respectively. Strains carrying pArray-1 showed high resistance against both T7 and P1
346 highlighting the additivity of phage resistance phenotypes. We then constructed pArray-2
347 containing *pic24* ($T7^R$) and bla_{OXA-10}, a class D β-lactamase gene that confers resistance against
348 carbenicillin (Figure 4B). The strain carrying pArray-2 showed high levels of resistance against
349 T7, and carbenicillin both separately and simultaneously (Figure 4B). Our results show that, as
350 predicted by the integron model, integrons can accumulate phage resistance phenotypes and
351 combine them with AMR, a capability that can have important implications for phage therapy.

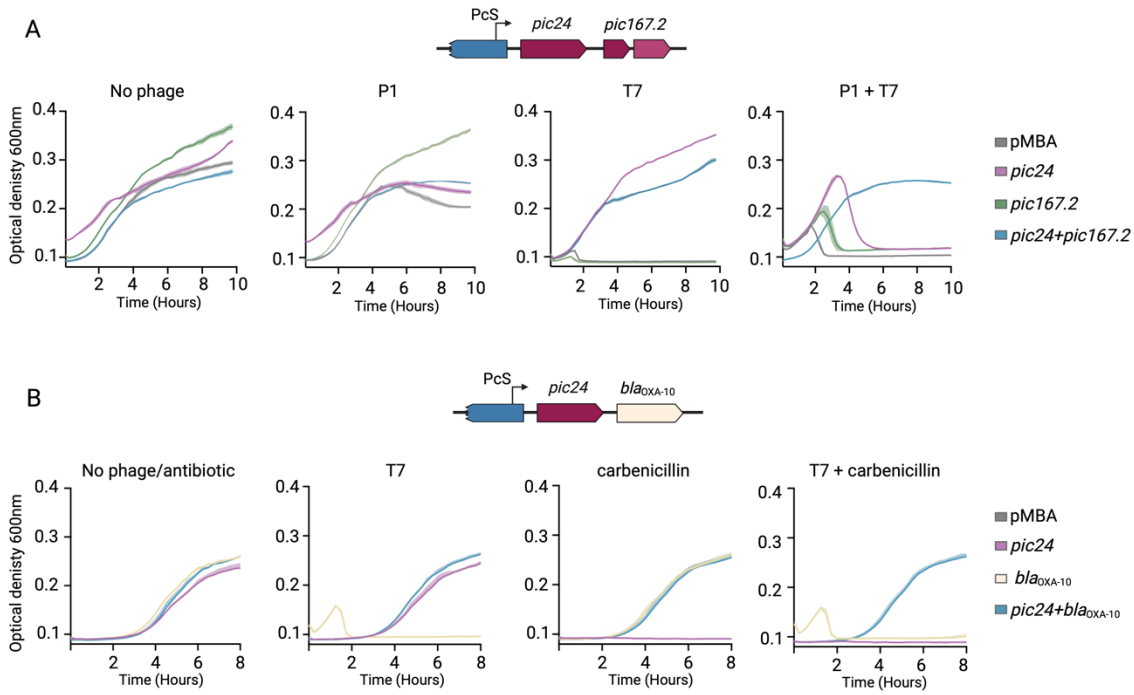

Figure 4. Additivity of Phage and Antibiotic Resistance Phenotypes in Multi-Cassette Arrays. Growth curves (OD_{600}) of *E. coli* strains containing **(A)** pMBA, *pic24* and *pic167.2* independently, and combined in an array*;* either with no phage, or challenged with phage P1, phage T7, and a combination of both. The array shows enhanced resistance to both phages compared to individual PICs, demonstrating the additive effect of multiple PICs within an integron; and **(B)** pMBA, *pic24* and bla_{OXA-10} independently, and combined in an array in the absence of phage or antibiotic, and challenged with phage T7, carbenicillin, and a combination of both. The combined array confers resistance to phage and antibiotics simultaneously. Growth curves are represented as the mean of three independent replicates. The standard error of the mean is represented as a lighter colour shade.

PICs entail different fitness effects that vary across species.

A major question in the field of phage defence is how these systems affect the fitness of the host. This has important implications in the accumulation of such systems in genomes and in their spread between species. Integrons are known to be low-cost platforms that can modulate the expression of the genes in their cargo by changing their position in the array [59–61]. Yet the net cost of each cassette can be different, which is of importance in their dispersal through HGT. To determine the cost of *pics*, we performed competition assays in both *E. coli* and *K. pneumoniae* using flow cytometry (Figure 5). Our results showed a broad distribution of fitness effects among PICs, ranging from large costs (ca. 40%) to virtually costless in both species. In *E. coli, pic217*, *pic128* and *picN* seemed to have a mildly positive impact in fitness (up to 3%) suggesting that acquisition of certain systems can be costless (Figure 5A). Interestingly, fitness effects were not conserved between genetic backgrounds. For instance, *picWGS21* entailed a small cost (ca. 7%) in *E. coli* but was very costly (ca. 30%) in *K. pneumoniae* (Figure 5B). Only

375 a few cassettes, like *picN* showed very similar cost in both species. The lack of cost of PICs in
376 certain genetic backgrounds, and the differences in fitness effects across backgrounds can be of
377 importance in the accumulation of cassettes and their preferential distribution of PICs among
378 species.

379 In the case of costly defence systems, a key advantage that integrons can provide,
380 compared to encoding them elsewhere, is that they can modulate their expression through the
381 shuffling of gene cassettes. Because the expression levels of genes and their fitness cost
382 generally correlate, we hypothesize that integrons can modulate the fitness of PICs in the array.
383 To test if the cost of a PIC can differ depending on the cassettes upstream, we compared the
384 cost entailed by *pic24* when located in first position of the array (see above) with the cost it
385 entails when encoded in third position (as it is found in the databases (Figure 2A)). For this, we
386 constructed an array (pArrayØ) containing two antibiotic resistance cassettes, *aacA54* and
387 *aacA8*, and introduced *pic24* downstream, as a third cassette (pArray-*pic24*). We have
388 previously shown that *aacA54* and *aacA8* have significant polar effects, strongly repressing the
389 expression of downstream cassettes[61]. Competition experiments show that while *pic24*
390 conferred a fitness cost of 11% when located in first position, it had no significant cost when in
391 third position (Figure 5C). This was due to the strong repression of its expression since phage
392 infection experiments showed pArray-*pic24* did not protect against T7 infection. Hence, costly
393 PICs can be carried by mobile integrons at no cost to be later reshuffled into first position,
394 providing phage resistance (*adaptation-) on demand*[62] We also show that PICs exert polar
395 effects on downstream cassettes (Figure 5D), participating in the modulation of function and
396 cost that we have previously demonstrated for resistance genes[61].
397

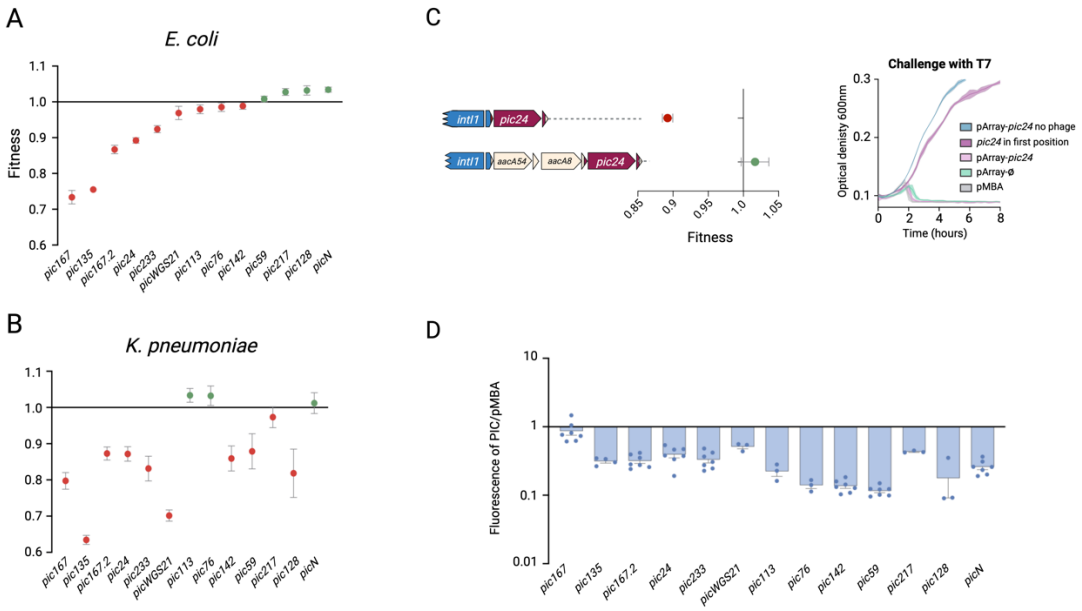

Figure 5. Fitness Effects of PICs. Fitness effects of PICs in **(A)** *E. coli* and **(B)** *K. pneumoniae*. Red circles represent fitness values below 1 (cost), while green circles indicate fitness values above 1 (gain). Fitness effects vary in sign and magnitude and are not conserved among genetic backgrounds. **(C)** Modulation of fitness cost and function by integron position. The graph shows the fitness effect of *pic24* in first position (competing pMBA vs pMBA-*pic24*) and third position (pArrayØ *vs.* pArray-*pic24*). The fitness cost imposed by the PIC is reduced in third position behind cassettes with strong polar effects. The cost is related to the function of the PIC since pArray-*pic24* does not confer resistance to T7. **(D)** Polar effects of PICs. All cassettes except *pic167* exert polar effects on downstream cassettes, limiting their expression. All assays have been performed at least three times. Error bars represent the standard error of the mean.

DISCUSSION

Phage therapy is an old approach with renewed interest in the light of the AMR crisis[63,64]. It allows for personalized treatments against multidrug resistant bacteria, with encouraging outcomes. Phage resistance is a rapidly evolving field of research. The constant discovery of new resistance genes, often encoded in defence islands and prophages, reveals the intense arms race between bacteria and their phages, and between mobile genetic elements. We lack knowledge on how defence systems are recruited into these islands and on their mobility, that seems to be somewhat limited[14]. In contrast, mobile integrons are highly adaptable genetic elements that have significantly contributed to the proliferation of multidrug resistance bringing to our hospitals a plethora of resistance cassettes from the genomes of environmental bacteria. Being shed to the environment at extremely high quantities (10^{23} per day)[65], mobile integrons have established a strong communication route between the genomes of pathogenic and environmental bacteria[66]. If new cassettes are adaptive, the rampant movement of mobile integrons among clinically relevant bacteria ensures a high speed of dissemination into our

424 hospitals. It is therefore critical for the future of phage therapy to understand the potential role
425 of integrons in phage defence. In this work we confirm that mobile integrons already contain
426 such systems.

427 We have successfully identified *pics* using bioinformatic tools and a phenotypic
428 screening with only T4 and T7 phages, and tested them against a panel of phages. As is the case
429 of most defence systems, *pics* displayed different specificities conferring narrow to broad
430 immunity in our assays. Nevertheless, because integrons can build arrays of cassettes, they can
431 combine phenotypes to confer multi-phage or phage-drug resistance, the same way they
432 currently confer multidrug resistance. In fact, *picN* is already found in an array with at least
433 three ARCs in a *P. aeruginosa* clinical isolate (Figure 2A). This, and other examples of arrays
434 containing *pic*s in different positions in the array, together with our results showing that PICs
435 can be carried at no cost, suggest that mobile integrons can become low-cost, highly-mobile
436 defence islands. An extreme case of this is shown by Darracq *et al*. in a back-to-back paper in
437 this issue, where they describe the presence of PICs in the Superintegron of *Vibrio cholerae*.
438 Indeed, in a recent work we have shown that the Superintegron is carried at no measurable cost
439 [67]. Additionally, their findings proves that chromosomal integrons are virtually infinite
440 repositories of PICs from where they can be recollected by mobile integrons. Both Darracq *et*
441 *al*. and us show that *pics* are functional in distant genetic backgrounds. In our work, we show
442 that this is the case in 3 of the 5 Gram negative species and strains of the ESKAPEE group of
443 highly resistant and dangerous pathogens: the kind of bacteria aimed by phage therapy assays.
444 This strongly suggests that the spread of PICs among them will be quick if selective pressure
445 with phages becomes commonplace. This has implications in what are today considered as
446 interesting therapeutic options. For instance, it is known that many *K. pneumoniae* phages bind
447 the bacterial capsule and that resistant clones can easily arise through capsule loss, albeit at the
448 cost of becoming non-virulent [68]. Hence, the acquisition of plasmids containing integrons with
449 *pics* can avoid this trade-off, rendering virulent clones resistant to phages and antibiotics at the
450 same time.

451 The role of mobile integrons in phage resistance exemplifies the interplay between
452 mobile genetic elements. Indeed, many of the PICs described here target the conjugative pilus
453 of *E. coli* IJ1862. Hence, plasmids containing integrons can indirectly benefit from the activity
454 of PICs that protect their host. Mobile Integrons would alleviate the trade-off between acquiring
455 adaptive traits encoded in the plasmid and the susceptibility to a variety of phages. Another
456 aspect of this complex interplay is the potential link of *pic128* with plasmid stability. Contrarily
457 to the *ddmABC* system, *pic128* does not interact with p15A plasmid or with any natural plasmids

458 present in Kp5. This result highlights that not all Lamassu systems have the same activity
459 toward plasmids. Given that horizontal gene transfer is key for bacteria to acquire plasmids
460 conferring resistance to antibiotics, it is possible that the lack of anti-plasmid activity of *pic128*
461 has been selected for in an environment with high antibiotic pressure.

462 Our work is not exempt of limitations. First, our screening -while successful in detecting
463 nine new genes- was based in the use of only T4 and T7. Given that some *pics* exhibit high
464 specificity against phages, it is likely that the number of *pic*s present in our collection of *gcus*
465 is underestimated. This could also apply to prophage-activation protection and plasmid stability
466 assays, if additional prophages and plasmids were tested. Additionally, algorithms to detect
467 defence systems are being constantly improved, so that detection of PICs in *gcus* will likely be
468 more prolific at the time this work is published.

469 This study shapes our perception of integrons. The presence of phage defence systems
470 and antibiotic resistance genes, proposes that integrons are protection elements against a large
471 breadth of environmental insults. This can guide the search for novel functions in the virtually
472 infinite reservoir of cassettes in nature. Our results have important implications in the field of
473 phage resistance, where mobile integrons provide extreme mobility at a very low and adjustable
474 fitness cost. Finding *pics* in Mobile integrons highlights the risk that phage resistance genes
475 follow the same dissemination route as ARG in the past century. The field of phage therapy
476 must be vigilant about the adaptive power of integrons since selective pressure will most likely
477 make them -again- a key player in (phage-) resistance. If the importance of integrons in the
478 evolution of phage resistance is neglected, it might come a day when phage hunting against
479 clinical isolates becomes extremely difficult.
480

481 **MATERIAL AND METHODS**

482 **Strains and Phage collection**

483 *E. coli* DH5a and *P. aeruginosa* PAO1 are laboratory strains. *K. pneumoniae* KP5 is a clinical
484 isolate. *E. coli* 594 [69], was kindly donated by José Penadés together with phages HK544 and
485 Φ80. Strains were grown at 37 °C in lysogeny broth (LB) or LB agar (1.5 %) (BD, France).
486 Zeocin was added at 100 µg/ml to maintain pMBA and pMBA-derived plasmids in *E. coli* and
487 *K. pneumoniae*. Tetracycline at 100 µg/ml was used to maintain pMBA plasmids in *P.*
488 *aeruginosa*. Liquid cultures were incubated in an Infors Multritron shaker at 200 rpm (Informs
489 HT, Swiss). Antibiotics were purchased from Sigma Aldrich (Merck, USA) except for zeocin
490 (InvivoGen, USA).

491 The coliphages included T4, T7, P1, MS2, G4, F1 which belong to the *Myoviridae*,
492 *Autographiviridae*, *Myoviridae*, *Fiersviridae*, *Microviridae* and *Inoviridae*, respectively. *E. coli*
493 phage MS2, F1, G4 and their host *E. coli* IJ1862 [47] were kindly provided by from Prof. James
494 J. Bull (University of Texas). Phages T4, T7, and P1 were purchased from the DMSZ collection
495 (Leibniz, Germany). The *K. pneumoniae* phage, named F13, (found in effluents from a hospital)
496 was selected for its ability to lyse a clinical isolate called Kp5, which produces the class D
497 carbapenemase OXA-48 and used as its host for this study. We computed the genomic data
498 obtained by Illumina technology with PHASTER to determined that F13 belongs to the
499 *Drexlerviridae* family. The *P. aeruginosa* PAO1 strain was used as a host for the Px4, Px5 and
500 Vs1 phages used in this study.

501 **Phage production**

502 We prepared phage solutions using previously published protocols [70]. Briefly, we grew host
503 bacteria in LB broth at 37ºC until they reached the exponential phase. At that point, we initiated
504 and monitored infection with the respective phage for 4 to 6 hours, depending on the specific
505 phage. When we observed a decrease in optical density (OD), we allowed the lysis process to
506 continue for an additional hour. We then transferred the cultures to polystyrene Falcon tubes for
507 centrifugation and subsequent filtration to collect the lysate containing the phage. Next, we
508 enumerated the phage solutions to determine the plaque-forming units (PFU). For plating, we
509 mixed bacterial cultures (OD_{600} ~1) with top agar medium and poured it onto agar dishes. After
510 allowing it to dry for 30 minutes, we spotted serial dilutions of the phages onto the agar plates
511 and incubated them overnight at 37ºC [71].

512 ***In silico* analysis**

513 We generated the list of *gcus* using the INTEGRALL database (INTEGRALL (ua.pt)) and
514 Integron finder [49,72]. To determine if the *gcus* associated with known phage resistance defense

515 systems, we subjected the sequences of all *gcus* to a BLAST search against the two main
516 defence system databases: DefenseFinder [73] and PADLOC [74]. For *gcus* that showed a resistance
517 phenotype but remained unidentified by these platforms, we used an AlphaFold2 pipeline
518 known as ColabFold for prediction, followed by Foldseek to gain insights into the protein
519 function of each *gcu* [75,76]. Additionally, we employed the Iterative Threading ASSEmbly
520 Refinement (ITASSER) platform to leverage complementary approaches for protein function
521 prediction [77].
522 We carried out the sequencing of the *K. pneumoniae* isolate Kp5 using a combination of
523 Illumina and Nanopore technologies, with SeqCoast (Portsmouth, USA) performing the
524 sequencing. We performed genome assembly using Unicycler software and conducted
525 subsequent analyses using the Center for Genomic Epidemiology platform. We determined the
526 resistome using the ResFinder web platform, identified the sequence type using MLST, and
527 characterized the plasmids using the PlasmidFinder web platform [78–80]. We assessed the
528 presence of prophages in the genome using the PHASTER web tool [81]. General DNA sequence
529 analysis was performed with Geneious and figures were created with BioRender.com.
530 **Cloning *gcu*s in pMBA**
531 All *gcus* were synthesized as double-stranded DNA by IDT ((Newark, USA), with an addition
532 of a 20 bp homology region corresponding to the targeted cloning site of pMBA located between
533 the *intI1* and *gfp* gene[33]. We performed the cloning process using the Gibson assembly method
534 [82] and selected clones on an LB agar plate supplemented with zeocin (25 µg/mL). We cloned
535 the entire sequences of the *gcus*, including the open reading frame (ORF) and their *attC* region,
536 into the pMBA vector. Our in-house designed pMBA plasmid contains a p15A replication
537 origin, a zeocin resistance marker, and a truncated intI1 gene followed by a *gfp* gene, acting as
538 a second integron cassette. We inserted the cloned *gcus* as the first cassette in the vector. To
539 ensure a relevant level of expression for each *gcu*, we selected the strongest version of the Pc
540 promoter, PcS, located within the *intI1* gene, for our constructions. For the construction of
541 pArray-1 and pArray-2, we cloned at second position of the integron-like structure of pMBA
542 the *pic167.2* or the $bla_{\text{OXA-10}}$ gene instead of having the *gfp* gene, respectively.
543 The construction of pArrayØ was accomplished using the Gibson assembly protocol, wherein
544 the *aacA54* and *aacA8* resistance gene cassettes were cloned into the pMBA-Δ*gfp* vector.
545 Subsequently, pArray-*pic24* was created by cloning the *pic24* gene into the third position of the
546 synthetic integron, downstream of the *aacA8* gene cassette.
547 For the cloning of *gcus* into *Pseudomonas aeruginosa* PAO1, we used a modified pMBA vector.
548 The p15A replication origin was replaced with the BBR1 origin to ensure replication in both

549 *E. coli* and *P. aeruginosa* species. Additionally, the strong PcS promoter was substituted with
550 its weaker version, PcW. Finally, a tetracycline resistance marker was introduced, as
551 *P. aeruginosa* exhibits low resistance to zeocin. The list of oligonucleotides used can be found
552 in Table S2.
553
554 **Growth curves and phage lysis monitoring**
555 We inoculated a single colony of a clone carrying a potential phage resistance gene into an
556 overnight culture of Luria Bertani (LB) broth at 37ºC. The next day, we adjusted the culture to
557 an optical density of 0.1 and transferred it to a 96-well plate containing LB broth supplemented
558 with zeocin (25 µg/mL). We then exposed the plate to different concentrations of phage to test
559 various multiplicities of infection (MOI). For all tested phages, we defined a high MOI
560 condition as an MOI of 1 and a low MOI condition as an MOI of 0,01. However, for phages T4
561 and T7, which exhibit high lytic activity, we set the high MOI condition to 0,01 and the low
562 MOI condition to 0,00001. We monitored growth curves using a Biotek HTX synergy plate
563 reader (Agilent, Madrid, Spain) at 600 nm over a 16-hour period. To assess the phage lysis
564 level, we calculated the area under the curve (AUC) for each growth condition, both with and
565 without phage as described previously [48]. The inhibition score for each sample was calculated
566 using the following formula:

567 $$Inhibition\ Score = \left(\frac{\Delta AUC}{\Delta AUC_{no\ phage}}\right) \times 100$$

568 where ΔAUC is the difference in AUC between the conditions with and without phage.
569 Specifically, $\Delta\mathrm{AUC} = \mathrm{AUC}_{no\ phage} - AUC_{phage}$. We calculated the inhibition scores for both
570 high and low multiplicity of infection (MOI) conditions. These scores were then normalized by
571 comparing them to the inhibition scores obtained from the control samples, which used the
572 empty pMBA vector. The normalization was done by computing the ratio of the inhibition score
573 of the experimental sample to the inhibition score of the control: $Inhibition =$
574 $\left(\frac{Inhibition\ Score_{pic}}{Inhibition\ Score_{pMBA}}\right) \times 100$. By using the "inhibition score", we normalize the reduction of the
575 area under the curve relative to growth without the phage. This allows for comparison of the
576 relative effects regardless of initial growth differences between strains.
577 **Prophage activation assay**
578 We chemically activate the lytic cycle of the prophages HK544 and Φ80 using mitomycin C at
579 a concentration of 0,05 µM. We then monitored the production of active phages over time by

580 taking 10 µL of the culture every two hours. After centrifugation, we performed serial dilutions
581 and spotted the phages on top agar plate to evaluate the phage concentration[83].

582 **Phage-resistant clone screening**

583 To identify new phage defence integron cassettes, we employed both liquid and solid media
584 screening strategies. Initially, we cultured clones carrying various *gcus* overnight in LB broth
585 with zeocin (25 µg/mL). The following day, a 1 OD dilution of each culture (10 µL) was spotted
586 onto LB agar plates supplemented with zeocin. After 1 hour of incubation, we applied 7 µL of
587 phage T4 solution at a concentration of 10^9 PFU/mL to the bacterial spots. After 16-18 hours of
588 incubation, we selected the clones that exhibited growth despite phage presence for further
589 analysis. Additionally, we conducted a high-throughput screening in 96-well plates, challenging
590 the entire *gcu* collection with phages T7 and T4 under two different multiplicities of infection
591 (MOI) conditions, following the protocol described previously.

592 **Plasmid stability experiment**

593 We co-transformed *E. coli* IJ862 with both the empty pMBA plasmid carrying the p15A replicon
594 and the L-arabinose inducible pBAD plasmid carrying either the *pic128* or *ddmABC* defence
595 system. For five days, three replicates were put in culture in LB broth supplemented with
596 carbenicillin (100 µg/ml) and L-arabinose (0,1%). Daily, we transferred 50 µl of each culture
597 into fresh 5 ml LB broth and used another 50 µl to count GFP-expressing colonies on LB agar
598 plates supplemented with carbenicillin.

599 To assess the stability of the endogenous clinical plasmids in Kp5 *K. pneumoniae* isolate, we
600 cultivated clones harbouring *pic128* in LB broth with zeocin (25 µg/ml) over five days. On days
601 1 and 5, we selected >120 colonies from LB zeocin agar plates and subcultured them onto
602 separate LB media containing either tetracycline (15 µg/ml), cefotaxime (50 µg/ml), or
603 ertapenem (30 µg/ml). This step aimed to detect any loss of resistance, which would suggest
604 the corresponding loss of one of the three natural plasmids.

605 ***attC* recombination experiments**

606 Recombination experiments were conducted as previously described[84]. Briefly, we cloned the
607 3' region of each *pic* pSW23T mobilizable plasmid containing a chloramphenicol resistance
608 marker into *E. coli* β2163 strain (*dapA*$^-$, *pir*$^+$) requiring diaminopimelic acid (DAP) to grow.
609 We used *E. coli* β2163 as donor strain for conjugation experiments using *E. coli* Dh5α strain
610 carrying a pBAD plasmid containing an L-arabinose inducible *intI1* gene and an *attI* site on its
611 chromosome as recipient. We performed conjugation experiments onto LB agar supplemented
612 with DAP and L-arabinose (0,1%) overnight. The next day, after cell recover, we performed
613 ten-folded dilutions onto LB agar supplemented with carbenicillin (100 µg/ml) and glucose

614 (0,1%) or with carbenicillin, glucose and chloramphenicol (25 µg/ml) to select for the total
615 population and recombinants, respectively.
616
617 **Fitness experiment**
618 To assess the fitness cost of each PIC, we performed *in vitro* competition assays following the
619 protocol described in [85] with some modifications. Briefly, we subcloned the panel of the nine
620 *pics* into a modified version of the pMBA vector, which includes a knock out *gfp* gene (with a
621 stop codon instead of the start codon), along with an empty vector control. We then subjected
622 this new set of clones to a fitness competition experiment against the wild type pMBA vector
623 carrying the intact *gfp* gene. Briefly, we grew six replicates of each clone overnight at 37ºC in
624 a 96-well plate filled with LB broth supplemented with zeocin (25 µg/ml). The next day, we
625 mixed cells containing the target *gcu* in the pMBA-Δ*gfp* in a 1:1 volume ratio with the clone
626 carrying the pMBA-WT vector. We diluted these mixtures 1:20 in 96-well plates containing
627 NaCl 0,9%. This plate was further diluted 1:20 in a plate with NaCl and another with LB broth
628 supplemented with zeocin. The first plate was used to estimate the percentage of pMBA-WT
629 and pMBA-*pic*-Δ*gfp* cells in the mixture on day 1, using a Cytoflex S cytometer (Beckman
630 Coulter, USA). The second plate (with LB) was incubated overnight. The next day these
631 cultures were diluted 1:400 in NaCl to determine the proportion of strains in the mixture as
632 explained above. Following the formula described in[85], fitness cost was calculated as the
633 difference in ratios of GFP-fluorescence between day 1 and day 2 for each *pic*.
634
635 **ACKNOWLEDGEMENTS**
636 We would like to thank Dr. José R. Penadés and Dr. James J. Bull for providing phages and
637 strains, and Tamara Barcos for technical assistance. We thank André Carvalho for critical
638 reading of the manuscript. NK is supported by funding from the European Union's Horizon
639 2020 research and innovation programme under the Marie Skłodowska-Curie grant agreement
640 No 847635 for the ANARC research project (No 4230415). The work in the MBA laboratory
641 is supported by the European Research Council (ERC) through a Starting Grant [803375];
642 Ministerio de Ciencia, Innovación y Universidades [BIO2017-85056-P]; Ministerio de Ciencia
643 e Innovación [PID2020-117499RB-100]; A.H. is supported by the PhD program at UCM. PB
644 is supported by the Juan de la Cierva program (FJC 2020-043017-I). P.D-C. was supported by
645 a Ramón y Cajal contract RYC2019-028015-I and the project PID2020-112835RA-I00, funded
646 by MCIN/AEI/10.13039/501100011033, ESF Invest in your future; MG-Q is supported by the
647 Subprograma Miguel Servet from the Ministerio de Ciencia e Innovación of Spain

(CP19/00104), Instituto de Salud Carlos III (Plan Estatal de I+D+i 2017–2020), and co-funded by European Social Fund "Investing in your future". J.A.E. is supported by the Atracción de Talento Program of the Comunidad de Madrid [2016-T1/BIO-1105, 2020-5A/BIO-19726];

REFERENCES

1. Antimicrobial Resistance Collaborators. Global burden of bacterial antimicrobial resistance in 2019: a systematic analysis. *Lancet* **399**, 629–655 (2022).
2. d'Herelle, F. Bacteriophage as a Treatment in Acute Medical and Surgical Infections. *Bull N Y Acad Med* **7**, 329–48 (1931).
3. Hatfull, G. F., Dedrick, R. M. & Schooley, R. T. Phage Therapy for Antibiotic-Resistant Bacterial Infections. *Annu Rev Med* **73**, 197–211 (2022).
4. Kortright, K. E., Chan, B. K., Koff, J. L. & Turner, P. E. Phage Therapy: A Renewed Approach to Combat Antibiotic-Resistant Bacteria. *Cell Host Microbe* **25**, 219–232 (2019).
5. Labrie, S. J., Samson, J. E. & Moineau, S. Bacteriophage resistance mechanisms. *Nat Rev Microbiol* **8**, 317–27 (2010).
6. Rostøl, J. T. & Marraffini, L. (Ph)ighting Phages: How Bacteria Resist Their Parasites. *Cell Host Microbe* **25**, 184–194 (2019).
7. Bernheim, A. & Sorek, R. The pan-immune system of bacteria: antiviral defence as a community resource. *Nat Rev Microbiol* **18**, 113–119 (2020).
8. Labrie, S. J., Samson, J. E. & Moineau, S. Bacteriophage resistance mechanisms. *Nat Rev Microbiol* **8**, 317–27 (2010).
9. Millman, A. *et al.* An expanded arsenal of immune systems that protect bacteria from phages. *Cell Host Microbe* **30**, 1556-1569.e5 (2022).
10. Millman, A. *et al.* An expanded arsenal of immune systems that protect bacteria from phages. *Cell Host Microbe* **30**, 1556-1569.e5 (2022).
11. Vassallo, C. N., Doering, C. R., Littlehale, M. L., Teodoro, G. I. C. & Laub, M. T. A functional selection reveals previously undetected anti-phage defence systems in the E. coli pangenome. *Nat Microbiol* **7**, 1568–1579 (2022).
12. Dedrick, R. M. *et al.* Prophage-mediated defence against viral attack and viral counter-defence. *Nat Microbiol* **2**, 16251 (2017).
13. Hochhauser, D., Millman, A. & Sorek, R. The defense island repertoire of the Escherichia coli pan-genome. *PLoS Genet* **19**, e1010694 (2023).
14. Makarova, K. S., Wolf, Y. I., Snir, S. & Koonin, E. V. Defense Islands in Bacterial and Archaeal Genomes and Prediction of Novel Defense Systems. *J Bacteriol* **193**, 6039–6056 (2011).
15. Ghaly, T. M. *et al.* The Natural History of Integrons. *Microorganisms* **9**, (2021).
16. Labbate, M., Case, R. J. & Stokes, H. W. The Integron/Gene Cassette System: An Active Player in Bacterial Adaptation. in 103–125 (2009). doi:10.1007/978-1-60327-853-9_6.
17. Mazel, D. Integrons: Agents of bacterial evolution. *Nat Rev Microbiol* **4**, 608–620 (2006).
18. Recchia, G. D. & Hall, R. M. Gene cassettes: A new class of mobile element. *Microbiology (N Y)* **141**, 3015–3027 (1995).

19. Partridge, S. R. *et al.* Definition of the attl1 site of class 1 integrons. *Microbiology (N Y)* **146**, 2855–2864 (2000).
20. Collis, C. M. & Hall, R. M. Expression of antibiotic resistance genes in the integrated cassettes of integrons. *Antimicrob Agents Chemother* **39**, 155–162 (1995).
21. Barraud, O. & Ploy, M. C. Diversity of class 1 integron gene cassette rearrangements selected under antibiotic pressure. *J Bacteriol* **197**, 2171–2178 (2015).
22. Souque, C., Escudero, J. A. & Maclean, R. C. Integron activity accelerates the evolution of antibiotic resistance. *Elife* **10**, 1–47 (2021).
23. Carvalho, A. *et al.* The expression of integron arrays is shaped by the translation rate of cassettes. doi:10.1101/2024.03.26.586746.
24. Guerin, É. *et al.* The SOS Response Controls Integron Recombination. *Science (1979)* **324**, 1034–1034 (2009).
25. Escudero*, J. A., Loot*, C., Nivina, A. & Mazel, D. The Integron: Adaptation On Demand. *Microbiol Spectr* **3**, (2015).
26. Partridge, S. R., Kwong, S. M., Firth, N. & Jensen, S. O. Mobile Genetic Elements Associated with Antimicrobial Resistance. *Clin Microbiol Rev* **31**, (2018).
27. Stokes, H. W. & Hall, R. M. A novel family of potentially mobile DNA elements encoding site-specific gene-integration functions: integrons. *Mol Microbiol* **3**, 1669–1683 (1989).
28. Domingues, S., da Silva, G. J. & Nielsen, K. M. Integrons: Vehicles and pathways for horizontal dissemination in bacteria. *Mob Genet Elements* **2**, 211–223 (2012).
29. Mazel, D. Integrons: agents of bacterial evolution. *Nat Rev Microbiol* **4**, 608–20 (2006).
30. Mitsuhashi, S., Harada, K., Hashimoto, H. & Egawa, R. On the drug-resistance of enteric bacteria. 4. Drug-resistance of Shigella prevalent in Japan. *Jpn J Exp Med* **31**, 47–52 (1961).
31. Kaushik, M., Kumar, S., Kapoor, R. K., Virdi, J. S. & Gulati, P. Integrons in Enterobacteriaceae : diversity, distribution and epidemiology. *Int J Antimicrob Agents* **51**, 167–176 (2018).
32. Hipólito, A., García-Pastor, L., Vergara, E., Jové, T. & Escudero, J. A. Profile and resistance levels of 136 integron resistance genes. *npj Antimicrobials and Resistance* **1**, 13 (2023).
33. Hipólito, A. *et al.* The expression of aminoglycoside resistance genes in integron cassettes is not controlled by riboswitches. *Nucleic Acids Res* **50**, 8566–8579 (2022).
34. Partridge, S. R., Tsafnat, G., Coiera, E. & Iredell, J. R. Gene cassettes and cassette arrays in mobile resistance integrons. *FEMS Microbiol Rev* **33**, 757–784 (2009).
35. Partridge, S. R., Tsafnat, G., Coiera, E. & Iredell, J. R. Gene cassettes and cassette arrays in mobile resistance integrons. *FEMS Microbiol Rev* **33**, 757–84 (2009).
36. Moura, A. *et al.* INTEGRALL: A database and search engine for integrons, integrases and gene cassettes. *Bioinformatics* **25**, 1096–1098 (2009).
37. Hipólito, A. *et al.* The expression of aminoglycoside resistance genes in integron cassettes is not controlled by riboswitches. *Nucleic Acids Res* **50**, 8566–8579 (2022).
38. Tesson, F. *et al.* Systematic and quantitative view of the antiviral arsenal of prokaryotes. *Nat Commun* **13**, 2561 (2022).
39. Payne, L. J. *et al.* PADLOC: a web server for the identification of antiviral defence systems in microbial genomes. *Nucleic Acids Res* **50**, W541–W550 (2022).

40. Hipólito, A. *et al.* The expression of aminoglycoside resistance genes in integron cassettes is not controlled by riboswitches. *Nucleic Acids Res* (2022) doi:10.1093/nar/gkac662.
41. Rousset, F. *et al.* Phages and their satellites encode hotspots of antiviral systems. *Cell Host Microbe* **30**, 740-753.e5 (2022).
42. Jaskólska, M., Adams, D. W. & Blokesch, M. Two defence systems eliminate plasmids from seventh pandemic Vibrio cholerae. *Nature* **604**, 323–329 (2022).
43. Duncan-Lowey, B. & Kranzusch, P. J. CBASS phage defense and evolution of antiviral nucleotide signaling. *Curr Opin Immunol* **74**, 156–163 (2022).
44. Haaber, J., Moineau, S., Fortier, L.-C. & Hammer, K. AbiV, a novel antiphage abortive infection mechanism on the chromosome of Lactococcus lactis subsp. cremoris MG1363. *Appl Environ Microbiol* **74**, 6528–37 (2008).
45. Matelska, D., Steczkiewicz, K. & Ginalski, K. Comprehensive classification of the PIN domain-like superfamily. *Nucleic Acids Res* **45**, 6995–7020 (2017).
46. Boyd, C. D. *et al.* Structural Features of the Pseudomonas fluorescens Biofilm Adhesin LapA Required for LapG-Dependent Cleavage, Biofilm Formation, and Cell Surface Localization. *J Bacteriol* **196**, 2775–2788 (2014).
47. Bull, J. J., Badgett, M. R., Springman, R. & Molineux, I. J. Genome properties and the limits of adaptation in bacteriophages. *Evolution (N Y)* **58**, 692 (2004).
48. Quinones-Olvera, N. *et al.* Diverse and abundant phages exploit conjugative plasmids. *Nat Commun* **15**, (2024).
49. Néron, B. *et al.* IntegronFinder 2.0: Identification and Analysis of Integrons across Bacteria, with a Focus on Antibiotic Resistance in Klebsiella. *Microorganisms* **10**, (2022).
50. Mazel, D. Integrons: agents of bacterial evolution. *Nat Rev Microbiol* **4**, 608–20 (2006).
51. Bouvier, M., Demarre, G. & Mazel, D. Integron cassette insertion: A recombination process involving a folded single strand substrate. *EMBO Journal* **24**, 4356–4367 (2005).
52. Bouvier, M., Ducos-Galand, M., Loot, C., Bikard, D. & Mazel, D. Structural features of single-stranded integron cassette attC sites and their role in strand selection. *PLoS Genet* **5**, e1000632 (2009).
53. Loot, C., Ducos-Galand, M., Escudero, J. A., Bouvier, M. & Mazel, D. Replicative resolution of integron cassette insertion. *Nucleic Acids Res* **40**, 8361–8370 (2012).
54. Bouvier, M., Ducos-Galand, M., Loot, C., Bikard, D. & Mazel, D. Structural features of single-stranded integron cassette attC sites and their role in strand selection. *PLoS Genet* **5**, e1000632 (2009).
55. Bouvier, M., Ducos-Galand, M., Loot, C., Bikard, D. & Mazel, D. Structural features of single-stranded integron cassette attC sites and their role in strand selection. *PLoS Genet* **5**, (2009).
56. Nivina, A., Escudero, J. A., Vit, C., Mazel, D. & Loot, C. Efficiency of integron cassette insertion in correct orientation is ensured by the interplay of the three unpaired features of attC recombination sites. *Nucleic Acids Res* **44**, 7792–7803 (2016).
57. MacDonald, D., Demarre, G., Bouvier, M., Mazel, D. & Gopaul, D. N. Structural basis for broad DNA-specificity in integron recombination. *Nature* **440**, 1157–1162 (2006).
58. Jaskólska, M., Adams, D. W. & Blokesch, M. Two defence systems eliminate plasmids from seventh pandemic Vibrio cholerae. *Nature* **604**, 323–329 (2022).

59. Lacotte, Y., Ploy, M.-C. & Raherison, S. Class 1 integrons are low-cost structures in Escherichia coli. *ISME J* **11**, 1535–1544 (2017).
60. Souque, C., Escudero, J. A. & MacLean, R. C. Integron activity accelerates the evolution of antibiotic resistance. *Elife* **10**, (2021).
61. Carvalho, A. *et al.* The expression of integron arrays is shaped by the translation rate of cassettes. 2 3 ORCID. doi:10.1101/2024.03.26.586746.
62. Escudero, J. A., Loot, C., Nivina, A. & Mazel, D. The Integron: Adaptation On Demand. *Microbiol Spectr* **3**, MDNA3-0019–2014 (2015).
63. Corbellino, M. *et al.* Eradication of a Multidrug-Resistant, Carbapenemase-Producing Klebsiella pneumoniae Isolate Following Oral and Intra-rectal Therapy With a Custom Made, Lytic Bacteriophage Preparation. *Clinical Infectious Diseases* **70**, 1998–2001 (2020).
64. Pirnay, J.-P. *et al.* Personalized bacteriophage therapy outcomes for 100 consecutive cases: a multicentre, multinational, retrospective observational study. *Nat Microbiol* **9**, 1434–1453 (2024).
65. Zhu, Y.-G. *et al.* Microbial mass movements. *Science (1979)* **357**, 1099–1100 (2017).
66. Gillings, M. *et al.* The evolution of class 1 integrons and the rise of antibiotic resistance. *J Bacteriol* **190**, 5095–5100 (2008).
67. Blanco, P. *et al.* Chromosomal Integrons are Genetically and Functionally Isolated Units of Genomes 2 3. doi:10.1101/2023.11.17.567518.
68. Song, L. *et al.* Phage Selective Pressure Reduces Virulence of Hypervirulent Klebsiella pneumoniae Through Mutation of the wzc Gene. *Front Microbiol* **12**, (2021).
69. Alqurainy, N. *et al.* A widespread family of phage-inducible chromosomal islands only steals bacteriophage tails to spread in nature. *Cell Host Microbe* **31**, 69-82.e5 (2023).
70. Bonilla, N. *et al.* Phage on tap-a quick and efficient protocol for the preparation of bacteriophage laboratory stocks. *PeerJ* **4**, e2261 (2016).
71. Ács, N., Gambino, M. & Brøndsted, L. Bacteriophage Enumeration and Detection Methods. *Front Microbiol* **11**, 594868 (2020).
72. Moura, A. *et al.* INTEGRALL: a database and search engine for integrons, integrases and gene cassettes. *Bioinformatics* **25**, 1096–8 (2009).
73. Tesson, F. *et al.* Systematic and quantitative view of the antiviral arsenal of prokaryotes. *Nat Commun* **13**, 2561 (2022).
74. Payne, L. J. *et al.* PADLOC: a web server for the identification of antiviral defence systems in microbial genomes. *Nucleic Acids Res* **50**, W541–W550 (2022).
75. van Kempen, M. *et al.* Fast and accurate protein structure search with Foldseek. *Nat Biotechnol* (2023) doi:10.1038/s41587-023-01773-0.
76. Mirdita, M. *et al.* ColabFold: making protein folding accessible to all. *Nat Methods* **19**, 679–682 (2022).
77. Yang, J. & Zhang, Y. Protein Structure and Function Prediction Using I-TASSER. *Curr Protoc Bioinformatics* **52**, (2015).
78. Bortolaia, V. *et al.* ResFinder 4.0 for predictions of phenotypes from genotypes. *Journal of Antimicrobial Chemotherapy* **75**, 3491–3500 (2020).
79. Carattoli, A. *et al. In Silico* Detection and Typing of Plasmids using PlasmidFinder and Plasmid Multilocus Sequence Typing. *Antimicrob Agents Chemother* **58**, 3895–3903 (2014).
80. Larsen, M. V. *et al.* Multilocus Sequence Typing of Total-Genome-Sequenced Bacteria. *J Clin Microbiol* **50**, 1355–1361 (2012).

81. Arndt, D. *et al.* PHASTER: a better, faster version of the PHAST phage search tool. *Nucleic Acids Res* **44**, W16–W21 (2016).
82. Avilan, L. Assembling Multiple Fragments: The Gibson Assembly. *Methods Mol Biol* **2633**, 45–53 (2023).
83. Ibarra-Chávez, R., Reboud, J., Penadés, J. R. & Cooper, J. M. Phage-Inducible Chromosomal Islands as a Diagnostic Platform to Capture and Detect Bacterial Pathogens. *Adv Sci (Weinh)* **10**, e2301643 (2023).
84. Bouvier, M., Demarre, G. & Mazel, D. Integron cassette insertion: a recombination process involving a folded single strand substrate. *EMBO J* **24**, 4356–4367 (2005).
85. DelaFuente, J., Rodriguez-Beltran, J. & San Millan, A. Methods to Study Fitness and Compensatory Adaptation in Plasmid-Carrying Bacteria. *Methods in Molecular Biology* **2075**, 371–382 (2020).